

Microwave frequency transfer over a 112-km urban fiber link based on electronic phase compensation

Wen-Xiang Xue(薛文祥), Wen-Yu Zhao(赵文宇), Hong-Lei Quan(全洪雷), Cui-Chen Zhao(赵粹臣), Yan Xing(邢燕), Hai-Feng Jiang(姜海峰), Shou-Gang Zhang(张首刚)

Citation: Chin. Phys. B . 2020, 29(6): 064209 . **doi:** 10.1088/1674-1056/ab84d6
Journal homepage: http://cpb.iphy.ac.cn; http://iopscience.iop.org/cpb

What follows is a list of articles you may be interested in

Spectral distortion of dual-comb spectrometry due to repetition rate fluctuation

Hong-Lei Yang(杨宏雷), Hao-Yun Wei(尉昊赟), Yan Li(李岩)

Chin. Phys. B . 2016, 25(4): 044207 . **doi:** 10.1088/1674-1056/25/4/044207

19-fs pulse generated by supercontinuum compression

Hua-Qiang Zhang(张华强), Peng Wang(王鹏), Wen-Jun Liu(刘文军), Yi-Lei Yao(姚翳蕾), Zhi-Jing Xu(徐志敬), Jian Li(李健)

Chin. Phys. B . 2016, 25(2): 024209 . **doi:** 10.1088/1674-1056/25/2/024209

Joint transfer of time and frequency signals and multi-point synchronization via fiber network

Nan Cheng(程楠), Wei Chen(陈炜), Qin Liu(刘琴), Dan Xu(徐丹), Fei Yang(杨飞), You-Zhen Gui(桂有珍), Hai-Wen Cai(蔡海文)

Chin. Phys. B . 2016, 25(1): 014206 . **doi:** 10.1088/1674-1056/25/1/014206

Optical coherence transfer over 50-km spooled fiber with frequency instability of 2×10^{-17} at 1 s

Ma Chao-Qun, Wu Li-Fei, Jiang Yan-Yi, Yu Hong-Fu, Bi Zhi-Yi, Ma Long-Sheng

Chin. Phys. B . 2015, 24(8): 084209 . **doi:** 10.1088/1674-1056/24/8/084209

Non-contact angle measurement based on parallel multiplex laser feedback interferometry

Zhang Song, Tan Yi-Dong, Zhang Shu-Lian

Chin. Phys. B . 2014, 23(11): 114202 . **doi:** 10.1088/1674-1056/23/11/114202

Microwave frequency transfer over a 112-km urban fiber link based on electronic phase compensation*

Wen-Xiang Xue(薛文祥)[1,2,3], Wen-Yu Zhao(赵文宇)[1,2], Hong-Lei Quan(全洪雷)[1,2,3], Cui-Chen Zhao(赵粹臣)[1,2,3], Yan Xing(邢燕)[1,2], Hai-Feng Jiang(姜海峰)[1,2], and Shou-Gang Zhang(张首刚)[1,2,†]

[1] *National Time Service Center, Chinese Academy of Sciences, Xi'an* 710600, *China*
[2] *Key Laboratory of Time and Frequency Primary Standards, Chinese Academy of Sciences, Xi'an* 710600, *China*
[3] *School of Astronomy and Space Science, University of Chinese Academy of Sciences, Beijing* 100049, *China*

(Received 3 February 2020; revised manuscript received 9 March 2020; accepted manuscript online 31 March 2020)

We demonstrate the transmission of a microwave frequency signal at 10 GHz over a 112-km urban fiber link based on a novel simple-architecture electronic phase compensation system. The key element of the system is the low noise frequency divider by 4 to differentiate the frequency of the forward signal from that of the backward one, thus suppressing the effect of Brillouin backscattering and parasitic reflection along the link. In terms of overlapping Allan deviation, the frequency transfer instability of 4.2×10^{-15} at 1-s integration time and 1.6×10^{-18} at one-day integration time was achieved. In addition, its sensitivity to the polarization mode dispersion in fiber is analyzed by comparing the results with and without laser polarization scrambling. Generally, with simplicity and robustness, the system can offer great potentials in constructing cascaded frequency transfer system and facilitate the building of fiber-based microwave transfer network.

Keywords: microwave frequency transfer, phase compensation, polarization mode dispersion

PACS: 42.62.Eh, 42.79.Sz, 06.30.Ft, 42.81.Uv **DOI:** 10.1088/1674-1056/ab84d6

1. Introduction

At present, the stability of the atomic frequency standards has reached an unprecedented level. In particular, cesium fountain clocks serving as primary frequency standards have demonstrated frequency instability of a few 10^{-16} at one-day integration time.[1,2] Meanwhile, comparing and synchronizing atomic clocks between distant laboratories with ultra-stable frequency transfer are essential in many fields of fundamental and applied science, such as time and frequency metrology, fundamental physics, particle accelerators, and astrophysics. However, the common methods for frequency transfer over satellite links to compare remote clocks are limited by an instability of 10^{-15} at one-day integration time,[3] which is insufficient to transfer modern atomic clocks.

Thanks to such factors as low attenuation, high reliability, and great potential for phase noise cancellation of optical fiber transmission,[4] as a result, the fiber-based ultra-stable optical frequency transfer,[5,6] the optical frequency comb signal transfer,[7,8] and the microwave frequency transfer[9–11] have all been investigated over the past decades. Although optical frequency transfer can provide an instability of 10^{-20} level at one-day integration time over an urban fiber of more than 100 km[6,12] and is insensitive to fiber attenuation, the optical frequency signal has to be converted to the required frequency by optical combs for most applications. The instability of fiber-based optical comb signal transfer is less than that of the optical frequency transfer. Furthermore, the pulse of the optical comb can be broadened seriously by fiber dispersion, resulting in a poor signal-to-noise ratio (SNR) of the output-detected signal. Consequently, optical comb signal is not suitable for long-distance transmission. With the advantage of simple architecture and convenience in use, microwave frequency transfer using intensity modulation of an optical carrier has demonstrated an instability much better than 10^{-18} at one-day integration time over urban fiber of about 80 km.[10,11] In 2010, a 9.15 GHz signal was transferred through an 86 km urban optical link with a frequency transfer instability of 1.3×10^{-15} at 1-s integration time and much better than 10^{-18} at one day using the optical compensation,[10] whose actuator, however, is complex and have small dynamic range, leading to limited applications of it. In 2012, a 9.1 GHz signal was transferred through an 80 km urban optical link with a frequency transfer instability of 7×10^{-15} at 1 s and 4.5×10^{-19} at one day using the electronic compensation.[11] Because of the same frequency used for both the forward and backward signals, the frequency transfer instability of the system is limited by Brillouin backscattering and parasitic reflections along the link, especially for long distance fiber link with more connectors and splices.

In this paper, we demonstrated the dissemination of a microwave frequency signal at 10 GHz over a 112-km urban fiber link based on a novel simple-architecture electronic compensation system. The key element of the system is the low noise frequency divider by 4 to differentiate the frequency of the for-

*Project supported by the National Natural Science Foundation of China (Grant Nos. 61825505, 91536217, and 61127901).
†Corresponding author. E-mail: szhang@ntsc.ac.cn
© 2020 Chinese Physical Society and IOP Publishing Ltd

ward signal from that of the backward one, thus distinguishing the main signal from the Brillouin backscattering and parasitic reflections along the link. To obtain high-resolution measurement of fiber link noise and facilitate construction of a cascaded frequency transfer system, microwave signals with high frequency are selected for the transferred and the reference signals. The effect of the polarization mode dispersion (PMD) in the fiber is analyzed by comparing the two cases with and without polarization scrambler (PS).

2. Architecture of the compensation system

In fiber-based frequency transfer, the propagation delay in forward and backward transmissions is approximately equal. Corresponding to phase or frequency variations of the transferred signals, the delay fluctuations can be measured by comparing the round-trip signal with the local signal. The architecture of the compensation system is shown in Fig. 1. With only frequency division and mixing, the frequency of the forward and backward signals is different and the link noise can be measured with great accuracy.

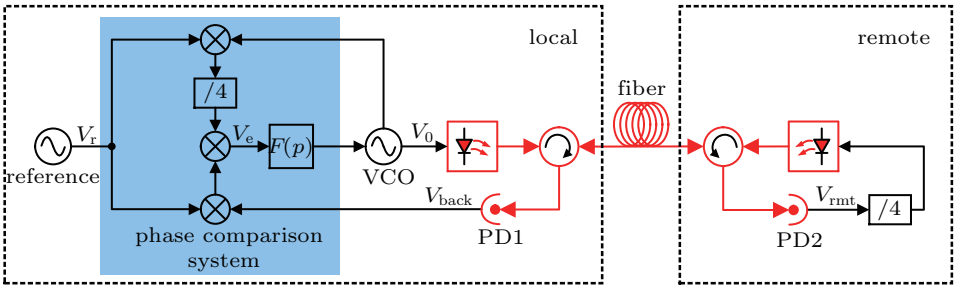


Fig. 1. Architecture of the compensation system for fiber-based microwave transfer. VCO: voltage-controlled oscillator; PD: photodiode.

The phase compensation in this system is theoretically analyzed as follows. At the local end, the reference signal V_r can be expressed as (without considering its amplitude)

$$V_r = \sin(\omega_r t + \varphi_r). \tag{1}$$

A voltage-controlled oscillator (VCO) generates a frequency signal V_0 that can be expressed as

$$V_0 = \sin(\omega_0 t + \varphi_0). \tag{2}$$

The frequency signal V_0 is transmitted in the fiber link using intensity modulation of the laser carrier. At the remote end, the incoming signal V_{rmt} detected by a fast photodiode (PD2) can be expressed as

$$V_{rmt} = \sin[\omega_0(t-\tau) + \varphi_0], \tag{3}$$

where τ is the one-way trip propagation delay of fiber. The V_{rmt} is frequency-divided by 4 to modulate the intensity of the second laser carrier, which is used to generate the backward signal. At the local end, the return signal V_{back} is detected by the second photodiode (PD1), which carries the round-trip phase fluctuations accumulated along the fiber. V_{back} can be expressed as

$$V_{back} = \sin\left[\frac{\omega_0(t-2\tau)}{4} + \frac{\varphi_0}{4}\right]. \tag{4}$$

After a series of electronic operations in the phase comparison system at the local end, an error signal V_e is given by

$$V_e = \sin\left[\left(\frac{2\omega_0 - 5\omega_r}{4}\right)t + \frac{2\varphi_0 - 5\varphi_r - 2\omega_0\tau}{4}\right]. \tag{5}$$

Equation (5) shows that the error signal covers not only the phase difference between the round-trip and reference signals, but also the difference between the VCO and reference signals. The error signal is processed in a loop filter ($F(p)$), and eventually used to correct the phase of transferred signal generated by VCO. When the $F(p)$ is closed, the V_e is equal to zero. Thus, it can be obtained that

$$\begin{cases} \omega_0 = 5\omega_r/2, \\ \omega_0\tau = \varphi_0 - 5\varphi_r/2. \end{cases} \tag{6}$$

As a result, the frequency signal V_0 is transformed into

$$V_0 = \sin\left(\frac{5}{2}\omega_r t + \frac{5}{2}\varphi_r + \omega_0\tau\right). \tag{7}$$

And the frequency signal V_{rmt} at the remote end becomes

$$V_{rmt} = \sin\left(\frac{5}{2}\omega_r t + \frac{5}{2}\varphi_r\right), \tag{8}$$

which is locked to the reference signal V_r. Thus, the link noise is compensated. It is interesting to note that any microwave frequency signal can be transmitted by this scheme as long as the frequency of V_0 is roughly 5/2 times that of V_r.

3. Experimental setup

The fiber link consists of two parallel 56-km fibers, which connects Lintong site and Chang'an site of the National Time Service Center (NTSC), both in Xi'an. We connect these two fibers using a bidirectional erbium-doped fiber amplifier (Bi-EDFA) with a gain of about 15 dB at Chang'an site to realize a 112-km urban link. The total loss of about 40 dB ($\sim$ 0.36 dB/km) indicates a poor quality of the fiber link.

The schematic diagram of the experimental system is shown in Fig. 2. Both the local and remote ends are located in the same laboratory at Lintong site. The reference frequency V_r is 4 GHz generated by an RF signal source (Keysight E8257D). In future experiments, the reference signal will be generated by ultra-stable photonic microwave source, which is phase locked to frequency standards and traceable to UTC(NTSC). The frequency of dissemination signal V_0 is 10 GHz.

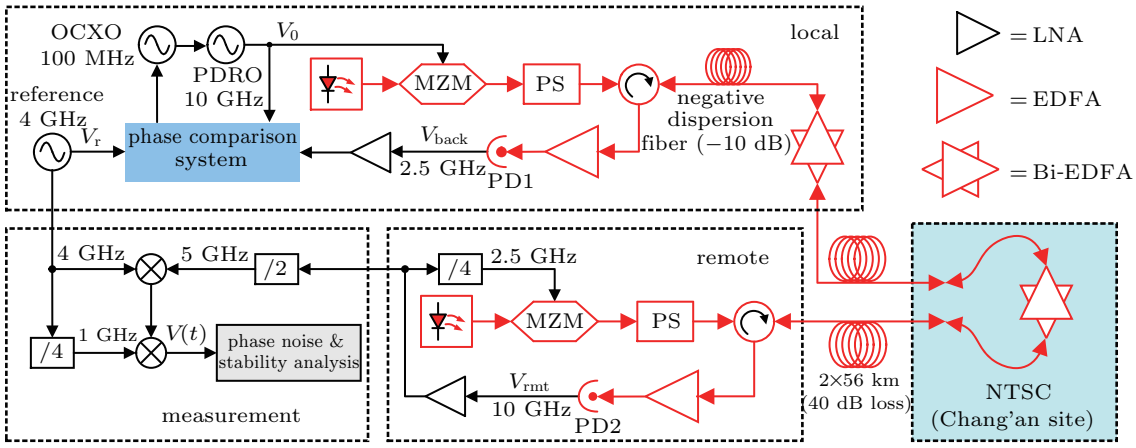


Fig. 2. Schematic diagram of the microwave frequency transfer system. OCXO: oven-controlled crystal oscillator; PDRO: phase-locked dielectric resonant oscillator; MZM: Mach–Zehnder modulator; PS: polarization scrambler; EDFA and Bi-EDFA: unidirectional and bidirectional erbium-doped fiber amplifier, respectively; LNA: low noise amplifier.

At the local end, the transferred frequency signal V_0 at 10 GHz is generated from a phase-locked dielectric resonant oscillator (PDRO), which is phase locked to a low noise 100-MHz oven-controlled crystal oscillator (OCXO). At the remote end, the incoming 10-GHz signal (V_{rmt}) is detected by PD2 and then is frequency-divided to 2.5 GHz with a low noise frequency divider by 4 (Analog Devices, HMC365). The 2.5-GHz signal is used to backward signal. Both microwave signals modulate the intensity of the distributed feedback laser diode (DFB-LD) at 1550 nm by Mach–Zehnder modulator (MZM). The 2.5-GHz backward signal is detected by PD1 at the local end, and the output signal V_{back} of PD1 carries the round-trip phase fluctuations accumulated over the fiber. As shown in the principle scheme (see Fig. 1), based on V_r, V_0, and V_{back}, the phase comparison system gives the control signal which is fed to 100-MHz OCXO to compensate the fiber link noise.

The performance of microwave frequency transfer over fiber link is degraded by PMD and chromatic dispersion.[9,10,13] Fortunately, the PMD effect can be averaged out by scrambling the polarization of the laser. Therefore, a polarization scrambler (PS) is inserted behind the MZM at each end. Each scrambler (Agiltron, NOPS-20) consists of a three-axis electromechanical polarization controller, and the output degree of polarization is less than 5%. To reduce the effect induced by the chromatic dispersion (~ 17 ps/nm·km) of optical fiber on frequency transfer, a large negative dispersion fiber (~ -1900 ps/nm) with a loss of about 10 dB is inserted at the local end. Behind the negative dispersion fiber, a Bi-EDFA with a gain of about 10 dB is used to compensate the optical loss caused by the negative dispersion fiber and to improve the SNR at detection.

4. Result and discussion

In order to evaluate the performance of frequency transfer, a heterodyne system[14] (see Fig. 2) is designed to measure the phase difference between the reference signal V_r and the received signal V_{rmt} in closed loop. In the measurement system, the 4-GHz reference signal V_r is power-split into two arms. In the first arm, the V_r is directly mixed with the 5-GHz signal generated from the V_{rmt} by a low noise frequency divider (Analog Devices, HMC364), so as to generate a 1-GHz signal. In the second arm, the V_r is frequency-divided to another 1-GHz signal by another low noise frequency divider (Analog Devices, HMC365). The phase difference between V_r and V_{rmt} is down converted to direct current (DC) voltage $V(t)$ by mixing the two 1-GHz signals and then measured by using a multimeter (Keysight, 3458A) with an effective measurement bandwidth of about 3 Hz. As a result, the propagation delay $x(t)$ is given by

$$x(t) = \frac{1}{\omega_0/2} \cdot \arcsin\left(\frac{V(t)}{V_{pp}/2}\right), \tag{9}$$

where V_{pp} is the peak-to-peak voltage of the $V(t)$ when the phase of V_r changes for 2π. The frequency transfer instability of the compensated link can be calculated from the $x(t)$. In addition, equations (7) and (8) show that the noise of the fiber link can be measured by mixing V_0 and V_{rmt} in closed loop.

Figure 3 shows the residual phase noise power spectral density (PSD) of the 112-km free-running and compensated optical link (black trace *a* and red trace *b*) at 10 GHz, which is measured by a fast Fourier transform (FFT) spectrum analyzer (Stanford Research System, SR785). Furthermore, it shows the noise of the 0-km compensated link (blue trace *c*), which

consists of an optical attenuator with an attenuation equivalent to 112-km fiber link. The free-running link noise is obtained by mixing V_0 and $V_{\rm rmt}$. The compensated link noise is obtained by measuring the noise of $V(t)$. The peak of the 112-km compensated link noise at about 260-Hz frequency offset is caused by the servo loop, which reveals that the compensated frequency bandwidth is less than $1/4\tau$ ($\sim$ 446 Hz) in agreement with Ref. [15].

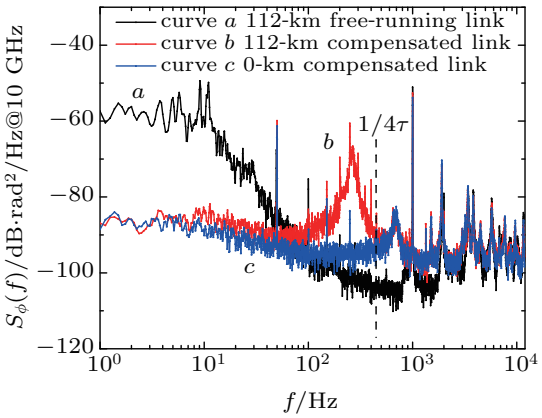


Fig. 3. The residual phase noise spectral density of fiber link measured at 10 GHz. Curve *a* 112-km free-running link; curve *b* 112-km compensated link; curve *c* 0-km compensated link.

Figure 4 shows the 112-km link propagation delay over 4.6 days without and with compensation (black trace and red trace, respectively). The propagation delay without compensation was obtained simultaneously with the compensation link signal by measuring the relative phase fluctuations between V_0 and $V_{\rm rmt}$. The compensation link propagation delay is about 400-fs peak-to-peak for 4.6 days. Comparable with the free-running link of about 13 ns, the rejection factor of the correction system is about 3250. The propagation delay of the 0-km compensated link (blue trace) is also plotted to indicate the limitation of the system, which results from replacing the 112-km fiber with an equivalent optical attenuator. Figure 5 shows the frequency transfer instability in terms of overlapping Allan deviation calculated from the propagation delay of the 112-km compensated link. An instability of 4.2×10^{-15} at 1-s integration time and 1.6×10^{-18} at one-day integration time (red circles) is obtained. The frequency instability of the 112-km free-running link (black squares) and the 0-km compensated link (blue triangles) is also plotted to highlight the effect of the compensation. It can be found that the medium- and long-term instability of the 112-km compensated link does not converge to the result of the 0-km link. Two main phenomena may degrade the performance of the 112-km compensated link. The first one is that microwave leakage may induce parasitic phase shifts.[16] The second limitation comes from conversion of amplitude-modulation noise (AM) into phase-modulation noise (PM) in photodiodes and mixers.[17–19] Nonetheless, the frequency transfer instability is much better than the performance of cesium fountain clocks.

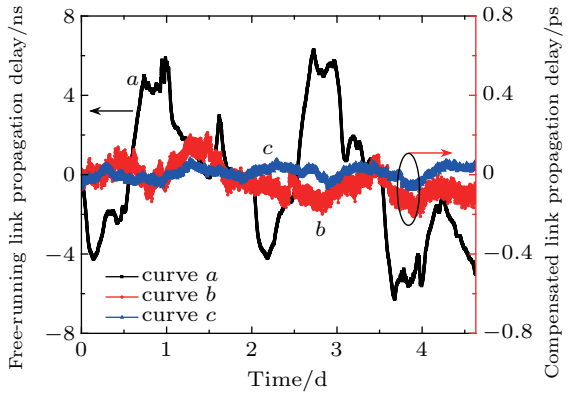


Fig. 4. The propagation delays of the 112-km free-running link (black trace *a*), the 112-km compensated link (red trace *b*), and the 0-km compensated link (blue trace *c*).

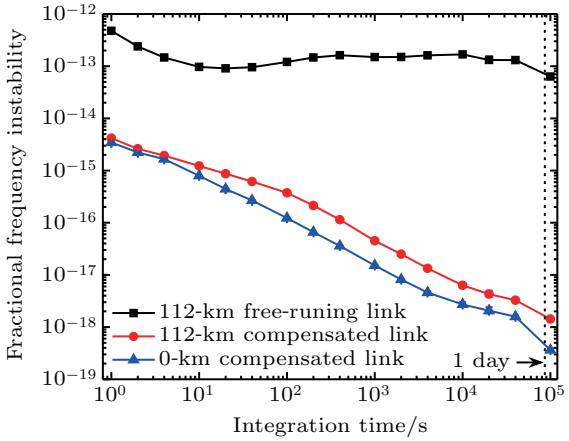


Fig. 5. Fractional frequency instability of the 112-km free-running link (black squares), the 112-km compensated link (red circles), and the 0-km compensated link (blue tri-angles).

As demonstrated in Refs. [9] and [10] the long-term instability is degraded by more than 1 order of magnitude due to the PMD in the optical compensation scheme. In order to evaluate the influence of the PMD, the propagation delay fluctuations of the compensated link without and with scrambler at each end are measured, as shown in Fig. 6. It can be seen that the scrambler has a slight effect on the delay fluctuations, but the correlation between the fiber propagation delay and air temperature is obviously decreased. The correlation coefficients are 0.454 and 0.013 without and with scrambler, respectively. Figure 7 shows the frequency instability without and with scrambler (black squares and red circles, respectively). When below 4000 s of integration time, there is little difference between the two results. When over 4000 s, the instability is slightly improved by the scrambler. These outcomes are due to the fact that the electronic compensator (an OCXO) causes much less polarization variation of the optical signals than the fiber stretcher used for the optical compensator.[12] On the other hand, the PMD coefficient of fiber is rather low ($\leqslant 0.1$ ps/$\sqrt{\rm km}$).[20,21] Consequently, in the electronic compensation scheme, the influence of the PMD is very limited. Thus, the system can operate well without any scrambler for the sake of economics and reliabilities.

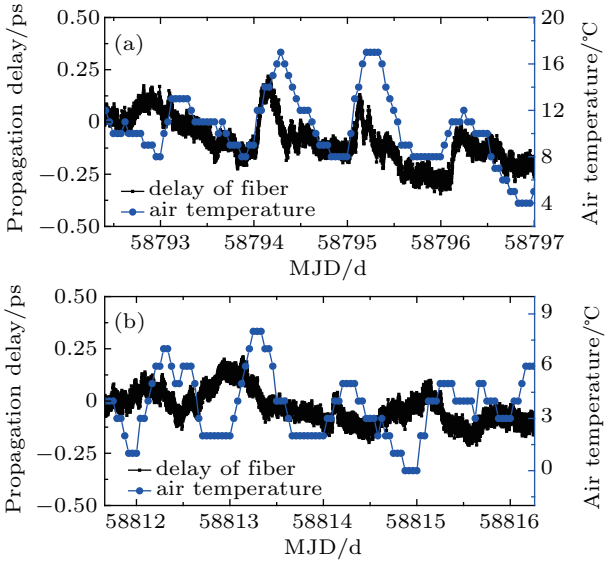


Fig. 6. Correlation between the fiber propagation delay and the air temperature: (a) without scrambler; (b) with scrambler. MJD: Modified Julian Date.

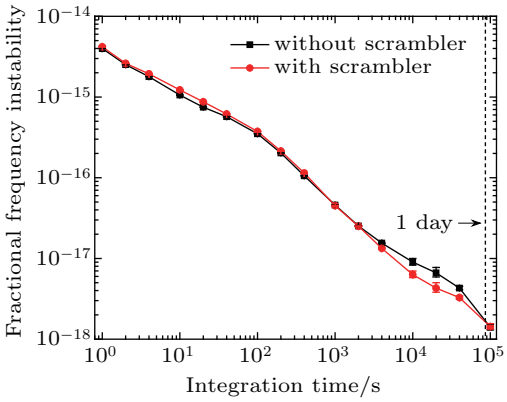


Fig. 7. Fractional frequency instability of the 112-km compensated link without (black squares) and with (red circles) scrambler.

5. Conclusion

Although the fiber-based microwave frequency transfer has been well developed by many groups, the design explored in this research is focused on reliable continuous operation at a high level over distances longer than 100 km and facilitating construction of a cascaded microwave transfer system, which is compatible with requirements of engineering application. We have demonstrated an ultra-stable microwave frequency transfer over a 112-km urban optical link as well as continuous long-term operation based on a novel electronic compensation system. A 10-GHz signal is transferred with a frequency transfer instability of 4.2×10^{-15} at 1-s integration time and 1.6×10^{-18} at one day, which is sufficient to transfer modern cold atom microwave frequency standards.

To compare atomic clocks with high precision in a longer distance and provide ultra-high precision frequency signal for more users, it is a wise choice to construct a network for ultra-stable frequency transfer by using cascaded transmission. Given its simple architecture, and especially considering the reference signal is also a microwave signal, the scheme proposed in this research is quite suitable for cascaded frequency transfer and then constructing fiber-based microwave transfer network.

Acknowledgment

The authors would like to thank Wenge Guo for his informative advice and to thank Xiaofei Zhang for his constructive suggestions on this paper.

References

[1] Guéna J, Abgrall M, Rovera D, Laurent P, Chupin B, Lours M, Santarelli G, Rosenbusch P, Tobar M E, Li R X, Gibble K, Clairon A and Bize S 2012 *IEEE Trans. Ultrason. Ferroelectr. Freq. Control* **59** 391

[2] Lipphardt B, Gerginov V and Weyers S 2017 *IEEE Trans. Ultrason. Ferroelectr. Freq. Control* **64** 761

[3] Bauch A, Achkar J, Bize S, Calonico D, Dach R, Hlavać R, Lorini L, Parker T, Petit G, Piester D, Szymaniec K and Uhrich P 2006 *Metrologia* **43** 109

[4] Ma L S, Jungner P, Ye J and Hall J L 1994 *Opt. Lett.* **19** 1777

[5] Jiang H F, Kéfélian F, Crane S, Lopez O, Lours M, Millo J, Holleville D, Lemonde P, Chardonnet C, Amy-Klein A and Santarelli G 2008 *J. Opt. Soc. Am. B* **25** 2029

[6] Deng X, Liu J, Jiao D D, Gao J, Zang Q, Xu G J, Dong R F, Liu T and Zhang S G 2016 *Chin. Phys. Lett.* **33** 114202

[7] Marra G, Slavík R, Margolis H S, Lea S N, Petropoulos P, Richardson D J and Gill P 2011 *Opt. Lett.* **36** 511

[8] Jung K, Shin J, Kang J, Hunziker S, Min C K and Kim J 2014 *Opt. Lett.* **39** 1577

[9] Lopez O, Amy-Klein A, Daussy C, Chardonnet C, Narbonneau F, Lours M and Santarelli G 2008 *Eur. Phys. J. D* **48** 35

[10] Lopez O, Amy-Klein A, Lours M, Chardonnet C and Santarelli G 2010 *Appl. Phys. B* **98** 723

[11] Wang B, Gao C, Chen W L, Miao J, Zhu X, Bai Y, Zhang J W, Feng Y Y, Li T C and Wang L J 2012 *Sci. Rep.* **2** 556

[12] Jiang H F 2010 *Development of ultra-stable laser sources and long-distance optical link via telecommunication networks*, Ph. D. Dissertation (Paris: Université Paris 13)

[13] Shen P, Gomes N J, Shillue W P and AlBanna S 2008 *J. Lightwave Technol.* **26** 2754

[14] Allan D W 1975 *The Measurement of Frequency and Frequency Stability of Precision Oscillators* (Washington: Nat. Bur. Stand., Tech. Note 669) p. 14

[15] Newbury N R, Williams P A and Swann W C 2007 *Opt. Lett.* **32** 3056

[16] Narbonneau F, Lours M, Bize S, Clairon A, Santarelli G, Lopez O, Daussy Ch, Amy-Klein A and Chardonnet C 2006 *Rev. Sci. Instrum.* **77** 064701

[17] Eliyahu D, Seidel D and Maleki L 2008 *IEEE Trans. Microwave Theory Tech.* **56** 449

[18] Cibiel G, Régis M, Tournier E and Llopis O 2002 *IEEE Trans. Ultrason. Ferroelectr. Freq. Control* **49** 784

[19] Nelson L M, Walls F L 1992 *Proceedings of the* 46*th IEEE Frequency Control Symp.*, May 27–29, 1992, Hershey, p. 831

[20] Schiano M 2004 *J. Opt. Fiber. Commun. Rep.* **1** 235

[21] Breuer D, Tessmann H J, Gladisch A, Foisel H M, Neumann G, Reiner H and Cremer H 2003 *Proceedings of the Dig. LEOS Summer Top. Meetings*, July 14–16, 2003, Vancouver, p. MB2.1/5–MB2.1/6